

INTERNATIONAL SOCIETY FOR SOIL MECHANICS AND GEOTECHNICAL ENGINEERING



This paper was downloaded from the Online Library of the International Society for Soil Mechanics and Geotechnical Engineering (ISSMGE). The library is available here:

<https://www.issmge.org/publications/online-library>

This is an open-access database that archives thousands of papers published under the Auspices of the ISSMGE and maintained by the Innovation and Development Committee of ISSMGE.

The paper was published in the proceedings of the 10th International Conference on Scour and Erosion and was edited by John Rice, Xiaofeng Liu, Inthuorn Sasanakul, Martin McIlroy and Ming Xiao. The conference was originally scheduled to be held in Arlington, Virginia, USA, in November 2020, but due to the COVID-19 pandemic, it was held online from October 18th to October 21st 2021.

Numerical Modeling of Scour around Mobile Objects with Prescribed Motion

Yalan Song,¹ Hassan Ismail,² and Xiaofeng Liu³

¹Department of Civil and Environment Engineering, Pennsylvania State University, University Park, PA 16802, USA; email: yxs275@psu.edu

²Department of Civil and Environment Engineering, Pennsylvania State University, University Park, PA 16802, USA; email: hxi33@psu.edu

³Department of Civil and Environment Engineering, Institute of Computational and Data Sciences, Pennsylvania State University, University Park, PA 16802, USA; email: xzl123@psu.edu

ABSTRACT

Stationary and mobile objects are ubiquitous in the subaqueous environment. Their existence disturbs the flow field and results in scour and erosion around them. Most previous research focused on the scour around stationary objects or ones with simple geometry, such as cylinders. Computer models typically have used the Arbitrary-Lagrangian-Eulerian (ALE) method to track the deforming bed. However, the ALE method cannot be easily used to deal with scour around mobile objects, such as boulders and unexploded ordnances (UXO). When objects are mobile, there are two moving boundaries (mobile objects and deformed bed). In most cases, these objects sit on the bed and thus the two moving boundaries may intersect and co-evolve. In this work, an immersed boundary (IB) method is adopted to capture the deformation of bed and motion of objects. The model is developed in the open source computational fluid dynamics platform OpenFOAM. In reality, the motion of objects is also controlled by other physical processes such as the movement of the granular bed. This work does not include the granular material physics, thus the motion of the objects is prescribed based on experimental observations. The simulation results are compared against flume experiments for both stationary and mobile objects.

INTRODUCTION

Abundant unexploded ordnances (UXO), including torpedoes, chemical weapons, and munitions dumps, exist underwater and threaten human health, safety, and the environment. Some of them are obsolete and have settled on the sea bed for many years. Many industries have to account for UXOs to assess the risks of water contamination or unexpected explosions (Howard et al., 2012). The prediction of munition mobility and dynamics is an essential factor for risk assessment and remediation action. Erosion and deposition change the distribution of sediment around objects, which means the granular supporting force from the bed is also changed. Thus, sediment transport is essential to impact munitions' mobility. For example, experiments have shown that munition may roll backward into the upstream scour hole instead of rolling downstream.

In this work, a 3D computational model was developed to predict the scour around mobile objects, to help determine the fate of potentially buried munitions. Most existing models can only simulate

scour near stationary objects with simple geometry, such as cylinders (Roulund et al., 2005), abutments (Bihs and Olsen, 2011), and simplified coastal structures (Liang et al., 2005). Typically, the Arbitrary-Lagrangian-Eulerian (ALE) method is utilized to track the bed deformation (Liu and Garcíá, 2008). However, this method is only useful for a simple and stationary structure. The simulation of scour and burial around mobile objects is still a challenge. Such models should include all processes in this problem, including turbulent flow, sediment transport, granular material dynamics, and six-degrees-of-freedom (6DoF) motion of objects. In this paper, the granular material dynamics is not included. Instead, the motion of objects is prescribed based on experimental observations. An immersed boundary (IB) method was used to capture both the bed deformation and the motion of objects.

NUMERICAL METHOD

The numerical scour model has two parts, i.e., hydrodynamic model and morphodynamic model. The scour model had been implemented in the open source computational physics platform OpenFOAM (OpenFOAM Foundation 2017). It is based on the existing immersed boundary method (Jasak et al., 2014; Jasak and Tuković, 2015).

In the hydrodynamic model, the flow is incompressible, viscous, and Newtonian. The governing equations, i.e., the Reynolds-averaged Navier-Stokes equations, can be written as:

$$\nabla \cdot \mathbf{u} = 0 \quad (1)$$

$$\frac{\partial \mathbf{u}}{\partial t} + \nabla \cdot (\mathbf{u}\mathbf{u}) = -\frac{1}{\rho} \nabla p + \nabla \cdot (\nu + \nu_t) \nabla \mathbf{u} \quad (2)$$

where \mathbf{u} is the flow velocity, p is the pressure, ν is the kinematic viscosity, and ν_t is the turbulent eddy viscosity. The $k - \omega$ SST-SAS model (SST-based Scale-Adaptive Simulation model) is used (Egorov and Menter, 2008) for turbulence closure.

To capture the moving boundaries (deforming bed and moving objects), an adaptive immersed boundary method is applied in this work. Instead of regenerating the mesh in each morphological step to conform to the moving boundaries, the boundary conditions are implemented by matrix manipulation of the governing equations. A Cartesian mesh is used as shown in Figure 1, where the computational domain is divided into three parts: IB cells, fluid cells, and solid cells. IB cells are defined as the closest cells to the immersed interface, Γ_{IB} , in the fluid region. For each IB cell, the intersection of the wall and the normal passing through the IB cell center (black crosses) is defined as a “hit point (HP)” (black circles). The point in the fluid region on the extended line normal to the immersed interface, Γ_{IB} , is defined as the “image point (IP)” (black triangles). These points are the main constructs used to determine the boundary condition of Γ_{IB} using a turbulent wall function (Roman et al., 2009).

In the immersed boundary method, the shear velocity, u_τ , is initially estimated as $C_\mu^{1/4} \sqrt{k_{IP}}$ and computed iteratively from:

$$u_\tau^{new} = \frac{u_{tan,IP}}{u_{IP,old}^+ (y_{IP}^+)} \quad (3)$$

where subscript IP denotes the value on the image point, subscript tan is the wall tangential value, and y_{IP}^+ is the dimensionless distance from IP to HP.

The values of flow variables on the image point, i.e., k_{IP} and $u_{tan,IP}$, are reconstructed by a quadratic polynomial interpolation using a stencil. The dimensionless velocity $u_{IP,old}^+$ is calculated with u_τ from the previous iteration and the wall function profile. The velocity on the IB cell center is calculated by the estimated u_τ from:

$$U_{IB}^{new} = \begin{cases} U_{IP} - \frac{1}{\kappa} u_\tau \log \left(\frac{y_{IP}}{y_{IB}} \right) & \text{if } y_{IB}^+ > y_{Laminar}^+ \\ u_\tau y_{IB}^+ & \text{if } y_{IB}^+ \leq y_{Laminar}^+ \end{cases} \quad (4)$$

Where κ is the von Karman constant equal to 0.41, and y_{IB} is the distance from IB cell center to HP. In this work, $y_{IP}/y_{IB} = 3$.

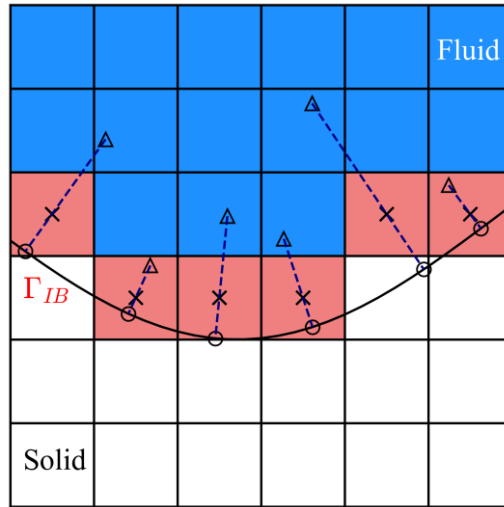


Figure 1. 2D schematic view of the immersed boundary method including the IB cell centers (black cross), hit points (black circles), image points (black triangles), IB cells (red filled), fluid cells (blue filled), and solid cell (white filled). The immersed interface, Γ_{IB} , is the black curve.

The morphodynamic model is restricted to the clear-water regime in which sediment suspension is negligible. Only bedload transport is included. The bed elevation is solved by the Exner equation

$$\frac{\partial z_b}{\partial t} = \frac{1}{1-n} (-\nabla \cdot \mathbf{q}_b) \quad (5)$$

where z_b is the bed elevation, n is the bed porosity, and \mathbf{q}_b is the bedload transport rate. The empirical bedload transport formula proposed in Engelund and Fredsøe (1976) is used to calculate \mathbf{q}_b .

RESULTS

The scour model is used to simulate two cases. The first case is the scour around a cylinder fixed on a cradle, which has also been experimentally studied in a flume. And the second case is a hypothetical case where a munition is freely placed on mobile bed.

In the first case, the cylinder is a simplification of a UXO with the same length ($L = 0.51$ m) and maximum diameter ($D = 0.09$ m) as shown in Figure 2.



Figure 2. Cylinder and the surrogate of a UXO.

The cradle is fixed to the flume bed and covered to a depth, H_s , of 0.12 m with sand (the median diameter of sand $d_{50} = 0.94$ mm) as shown in Figure 3. The cylinder rests on the cradle at the sand-water interface. The channel has a water depth, H_w , of 0.4 m and mean velocity, U , of 0.22 m/s.

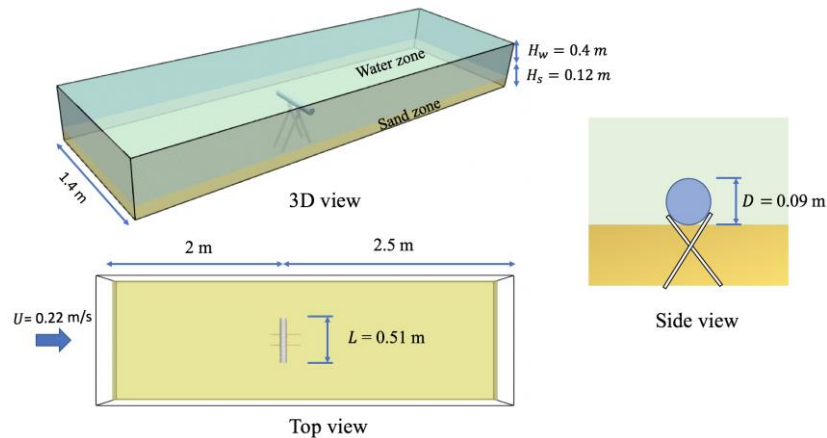


Figure 3. Setup for the simulation of scour around a cylinder on a cradle.

Figure 4 shows the bed elevation at the equilibrium. The flow condition and the object are symmetric along the center plane of the channel. The simulation and experimental results of bed elevation are also symmetric and shown in the same figure for a better comparison. The upper panel is the simulation result and the lower panel is the experimental result. The red dash line denotes the position of cylinder. The erosion begins under the two ends in the cross-channel direction of cylinder and expands along the upstream-facing edge of the cylinder toward the center until the two scour holes merge together. Then, the scour hole deepens and undermines the sand

around the cradle. The exposure of cradle increases the flow velocity around them as well as the erosion. As a result, the deepest scour occurs around the cradle arms, which is reflected in both the simulation and experimental results. It can be observed from Figure 4 that the scour hole under the cylinder was well captured by the model. The simulated deposition height behind the cylinder is lower than the experiment because the fluid and sediment mesh far downstream are relatively coarse to maintain computational efficiency.

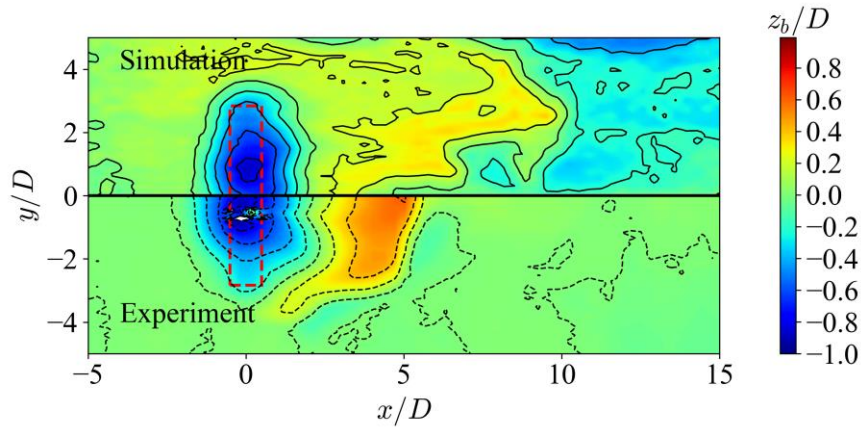


Figure 4. Comparison of bed elevation at equilibrium for scour around a cylinder on a cradle. The upper panel is from the simulation and the lower panel is from the experiment.

The second case is the simulation of scour around a mobile munition initially laying on an erodible bed. The simulation setup is shown in Figure 5. The channel has a water depth, H_w , of 0.2 m and sand depth, H_s , of 0.1 m. The inlet velocity U is 0.5 m/s and the median diameter d_{50} of the sand is 0.26 mm. The munition, which has a maximum length, L , of 194 mm and maximum diameter, D , of 51 mm, is assumed to move vertically downward with a velocity of 0.4 mm/s.

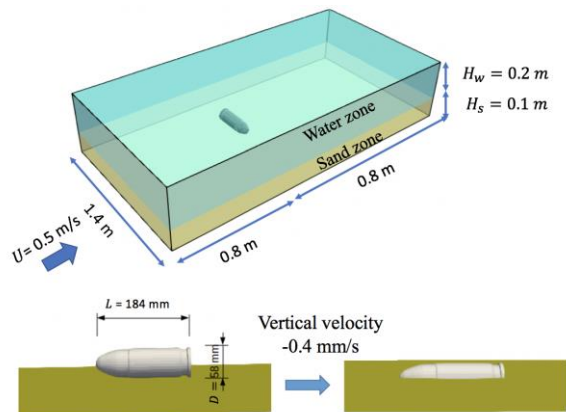


Figure 5. Setup for simulation of scour around a munition sitting on a sediment bed.

Figure 6 shows the bed elevation at the equilibrium of the second case. The projection of the munition is marked with grey. The incoming flow decelerates due to the presence of the munition

leading to concentrated deposition just upstream of the munition. Erosion occurs immediately downstream of the munition, with the deepest scour downstream of the broadest part of the munition. Additionally, there is no scour under the munition. As the erosion begins below narrower parts of the munition (the tip or the narrow circle near the broad end of the munition), the munition's prescribed downward motion fills the developed void. At the same time, the sand under the munition is pushed to the surroundings of munition. The deformation of the bathymetry changes the distribution of sediment as well as the granular forces acting on the munition. In future work, the prescribed motion of the objects will include a full six-degrees-of-freedom motion from experimental observations. Then, the relationship between bed deformation bathymetry and the munition's movement can be investigated.

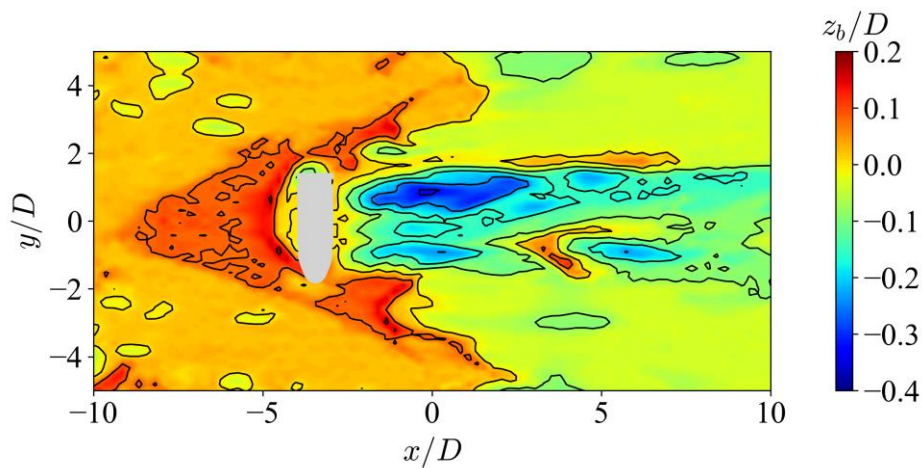


Figure 6. Simulation result of bed elevation at equilibrium for scour around a mobile munition.

CONCLUSION

A 3D computational scour model for stationary and mobile objects was developed. The immersed boundary method had been successfully implemented to capture both bed deformation and the motion of objects. The model was used to simulate two cases: scour around a fixed cylinder and scour around a mobile munition on an erodible bed. In the first case, the model predicted the process of erosion well and captured the shape of the scour hole around the cylinder. In the second case, erosion mainly occurred in the downstream region because the scour hole under the munition was filled by the munition's prescribed downward motion.

ACKNOWLEDGEMENT

This work was supported by the Strategic Environmental Research and Development Program (SERDP, Award Number W74RDV70063408).

REFERENCE

- Bihs, H. and Olsen, N.R.B., 2011. Numerical modeling of abutment scour with the focus on the incipient motion on sloping beds. *Journal of Hydraulic Engineering*, 137(10), pp.1287-1292.
- Egorov, Y. and Menter, F., 2008. Development and application of SST-SAS turbulence model in the DESIDER project. In *Advances in Hybrid RANS-LES Modelling* (pp. 261-270). Springer, Berlin, Heidelberg.
- Engelund, F. and Fredsøe, J., 1976. A sediment transport model for straight alluvial channels. *Hydrology Research*, 7(5), pp.293-306.
- Greenshields CJ. *OpenFoam User Guide*, V5. 0. OpenFOAM foundation Ltd. 2017 Jul.
- Howard, B., Aker, J. and Reid, M., 2012. Risk management for unexploded ordinance (UXO) in the marine environment. *Dalhousie Journal of Interdisciplinary Management*, 8(2).
- Jasak, H., Rigler, D. and Tuković, Ž., 2014. Design and implementation of Immersed Boundary Method with discrete forcing approach for boundary conditions. In *11th World Congress on Computational Mechanics, WCCM 2014, 5th European Conference on Computational Mechanics, ECCM 2014 and 6th European Conference on Computational Fluid Dynamics, ECFD 2014* (pp. 5319-5332). International Center for Numerical Methods in Engineering.
- Jasak, H., and Tuković, Ž., 2015. *Immersed Boundary Method in FOAM - Theory, Implementation and Use (Presentation Slides)*.
- Liang, D., Cheng, L. and Li, F., 2005. Numerical modeling of flow and scour below a pipeline in currents: Part II. Scour simulation. *Coastal engineering*, 52(1), pp.43-62.
- Liu, X. and García, M.H., 2008. Three-dimensional numerical model with free water surface and mesh deformation for local sediment scour. *Journal of waterway, port, coastal, and ocean engineering*, 134(4), pp.203-217.
- Roman, F., Napoli, E., Milici, B., & Armenio, V. (2009). An improved immersed boundary method for curvilinear grids. *Computers & fluids*, 38(8), 1510-1527.
- Roulund, A., Sumer, B.M., Fredsøe, J. and Michelsen, J., 2005. Numerical and experimental investigation of flow and scour around a circular pile. *Journal of Fluid Mechanics*, 534, pp.351-401.